PFC/JA-92-6

# A Fusion-Product Source

K. W. Wenzel, D. H. Lo, R. D. Petrasso, J. W. Coleman,

C. K. Li, J. R. Lierzer, C. Borrás, T. Wei,

E. Hsieh† and T. Bernat†

Submitted for publication in: *Review of Scientific Instruments*

**Plasma Fusion Center**

**Massachusetts Institute of Technology**

Cambridge, MA 02139

**† Lawrence Livermore National Laboratory**

Livermore, CA 94550

This work was supported in part by U.S. DOE Grant No. DE-FG02-91ER54109

and LLNL Subcontract No. B116798.

# A Fusion-Product Source

**K. W. Wenzel[†], D. H. Lo[‡], R. D. Petrasso, J. W. Coleman, C. K. Li, J. R. Lierzer, C. Borrás, and T. Wei**
*MIT Plasma Fusion Center, Cambridge MA 02139*

**E. Hsieh and T. Bernat**
*Lawrence Livermore National Laboratory, Livermore CA 94550*

March 1992

**Abstract**

We refurbished a Texas Nuclear Cockcroft-Walton neutron generator for use as a general fusion-product source. This well-calibrated source is now used routinely for characterizing energetic charged-particle detectors, for the development of nuclear fusion diagnostics, for studying radiation damage, and for calibrating x-ray detectors for laboratory and space plasmas. This paper is an overview of the facility. We describe the main accelerator operating systems, the primary fusion reactions studied, and several diagnostics used to characterize the fusion-product source.

## I. Introduction

The cornerstone of our fusion-product facility is a 170-kV Cockcroft-Walton linear accelerator, located in a radiation vault area with ~3-foot thick concrete walls. Originally manufactured (circa 1962) by Texas Nuclear Corp. (TNC), it is described in Ref. 1. Over the past two years we have refurbished the accelerator in order to use it as a well-calibrated source of fusion products and Particle-Induced X-Ray Emissions (PIXE; described in Ref. 2). In this paper, we emphasize its use as a fusion-product source.

We describe in Section II its main components: the target chambers, the vacuum/gas system, and the ion source. Fusion-product generation is described in Section III, and in Section IV we discuss diagnostics used to characterize the emitted radiations.

## II. Accelerator Systems

The TNC device was originally a neutron generator without any direct access to the target vacuum, thereby precluding, for example, the detection of charged fusion products. Our most significant change was to build two new target chambers that allowed detectors to "see" the target, either directly in vacuum or in air through thin windows[3] (see Fig. 1).

The beam is limited by a 1-cm-diameter stainless-steel collimator, electrically insulated from the drift tube, located about 15 cm upstream from the target. The collimator is biased at +300 V to attract secondary electrons

created at the collimator edge. Beam current on target is measured by a micro-ammeter connected between the target and ground. The water-cooled target is biased at +200 V to attract secondary electrons generated at the target surface and thus avoid misleading current measurement. The target chamber may be separated from the beam line by a gate valve to allow target changes without bringing the entire accelerator to air.

Vacuum is maintained by a Leybold TMP150V turbomolecular pump (which replaces the original ion pump). The base pressure is $\sim$0.5-1.0$\times 10^{-6}$ torr, and the operating pressure ranges from $5 \times 10^{-6}$ to about $5 \times 10^{-5}$ torr depending on beam power, target conditions, and the particular diagnostics installed (*e.g.*, vacuum is degraded when we use an ultra-thin-window gas-flow proportional counter to measure low energy x rays).

We use high-purity, research-grade gases (H, D, $^3$He, and $^4$He) as beam species, which are fed through electrically insulating tubing to the high-voltage section of the accelerator via a Granville-Phillips 203 variable leak valve. (This replaces the original resistively-heated Pd leak, which only passed hydrogen isotopes.)

The ion source consists of a plasma bottle, an extraction electrode, a compression solenoid, and a focus electrode. Plasma is generated in the bottle by 60-MHz RF rings. Ions are forced from the bottle by application of up to +5 kV on the extraction electrode. The magnetic field from the solenoid compresses the plasma and optimizes molecular break-up and gas

ionization.[1] After extraction, some beam focusing is achieved by applying up to -10 kV on a focus electrode located just downstream from the ion source. Subsequently the beam is accelerated down the column to the drift tube which houses the target.

## III. Fusion-Product Generation

D-D or D-$^3$He reactions are generated by accelerating D or $^3$He ions onto a deuterated titanium or deuterated erbium target (accelerating voltage $\lesssim$170 kV; beam current $\lesssim$300 $\mu$A):

$$\mathrm{D} + \mathrm{D} \longrightarrow p(3.0\ \mathrm{MeV}) + \mathrm{T}(1.0\ \mathrm{MeV}) \tag{1}$$

$$\mathrm{D} + \mathrm{D} \longrightarrow n(2.5\ \mathrm{MeV}) + {}^3\mathrm{He}(0.8\ \mathrm{MeV}) \tag{2}$$

$$\mathrm{D} + {}^3\mathrm{He} \longrightarrow p(14.6\ \mathrm{MeV}) + \alpha(3.7\ \mathrm{MeV}) \tag{3}$$

The maximum reaction rates, normalized to the beam current, are $R_{\mathrm{DD}} \simeq 9 \times 10^5/(s\ \mu\mathrm{A})$ and $R_{\mathrm{D^3He}} \simeq 3 \times 10^4/(s\ \mu\mathrm{A})$. In the future we will implement a third target chamber for tritiated targets in order to generate 14.1-MeV neutrons through D-T fusion:

$$\mathrm{D} + \mathrm{T} \longrightarrow n(14.1\ \mathrm{MeV}) + \alpha(3.5\ \mathrm{MeV}). \tag{4}$$

The particle energy observed in the laboratory depends on the beam energy and the angle of observation, $\theta$, relative to the beam direction (see Fig. 1). This kinematic effect makes possible a "tunable" source of monoenergetic particles. (Figs. 2 and 3 show examples.)

## IV. Cockcroft-Walton Diagnostics

Our standard charged-fusion-product diagnostic uses silicon surface-barrier diodes (SBDs) inside vacuum (VSBD), viewing the target at 120°. SBDs have intrinsic detection efficiency of 1.0 and energy resolution of $\lesssim$50 keV for most charged particles, which is sufficient to uniquely identify the charged products of reactions (1)–(3). Thus VSBD provides an absolute calibration of the fusion rate, which was not available with the original target chamber.[1]

We typically use a partially-depleted SBD covered with a 1.5-$\mu$m-mylar filter to protect it from backscattered beam particles. However, this precludes the detection of 0.8-MeV D-D $^3$He particles, because they lose most of their energy in the mylar.[4] Another limitation of partially-depleted SBDs (typical thickness $\sim$300 $\mu$m) is that they cannot measure the *full energy* of the 14.6 MeV D-$^3$He proton (its range is about 1300 $\mu$m in silicon[5]). In order to measure this, a 2000-$\mu$m thick fully-depleted SBD is used.

We are also examining the charged particle emission at other values of $\theta$. For example, Fig. 2 shows spectra of D-D fusion products taken with VSBD at $\theta \simeq 65°$ and $\theta \simeq 115°$. The energy of both the proton and triton shifted downward as $\theta$ was increased.

The relative neutron flux is monitored with a $^3$He or $BF_3$ thermal-neutron detector inside a moderating cylinder located a fixed distance from the target. Around the target chamber the time-integrated fast- and thermal-neutron doses are also monitored with neutron dosimeters. These detectors provide

a quantitative comparison of the total number of neutrons produced during different experiments. This is important for radiation damage experiments, where the total dose on a sample is the important parameter.

We have used both $^3$He and $^4$He proportional counters to measure fast neutron spectra. Fig. 3 shows $^3$He proportional-counter fast-neutron spectra taken at $\theta \simeq 40°$ and $\theta \simeq 140°$. For incident neutrons with energy $E_n$, each spectrum consists of three primary features:[6] (1) the thermal peak (TP at the capture reaction Q-value, 765 keV) and the corresponding wall-effect contributions; (2) the $^3$He recoil edge at 75% of $E_n$ (RE); and (3) the fast neutron capture peak (FP at Q + $E_n$). Table 1 compares the measured fast neutron energies with the values calculated based on kinematics for $\theta$ = 40°, 90°, and 140°. The measured and calculated neutron energies agreed to within about 5%.

X rays are generated in the Cockcroft-Walton via two mechanisms. First, PIXE generates characteristic line radiation from the target material (typically with energy <20 keV)[3]. Second, a very much smaller but undesired x-ray flux is generated near the ion source when secondary electrons are accelerated back up to the high voltage section, generating high-energy bremsstrahlung in the process.

We measure PIXE x-ray spectra with a Si(Li) detector for x rays with energy $\gtrsim$1 keV, and thin-window gas-flow proportional counters for x rays with energy $\lesssim$1.5 keV.[3] We also monitor x rays from secondary electrons

using both active (electronic) and passive x-ray detectors. As passive x-ray detectors, we use x-ray dosimeters located around the accelerator room. These monitors are read and recorded before and after each run. As an active x-ray detector, we use a Centronic IG1 ionization chamber located near the ion source.

The accelerator generates $\gamma$ rays via low-probability branches of fusion reactions (*e.g.*, $^{3}$He(D,$\gamma$)$^{5}$Li, $^{11}$B(p,$\gamma$)$^{12}$C or $^{7}$Li(p,$\gamma$)$^{8}$Be). These reactions are used as well-calibrated high-energy $\gamma$-ray sources for characterizing $\gamma$-ray diagnostics,[7] such as NaI(Tl) scintillators or a High-Purity Germanium high-resolution spectrometer. As an illustration, Fig. 4 shows the $\gamma$-ray spectrum taken with a NaI(Tl) scintillator from the $^{7}$Li(p,$\gamma$)$^{8}$Be reaction.

## Acknowledgements

Dr. Ramon Leeper and Dr. Carlos Ruiz of Sandia National Laboratory and Dr. Lynn Provo of General Electric provided several deuterated erbium targets used in this work. We appreciate Dr. Fredrick Seguin's careful reading of the manuscript. This work was supported by LLNL Subcontract B116798, U.S. DOE Grant No. DE-FG02-91ER54109, by the U.S. DOE Fusion Energy Postdoctoral Fellowship†, and by the U.S. DOE Magnetic Fusion Energy Technology Fellowship‡.

1. J. T. Prud'homme, *Texas Nuclear Neutron Generators*, Texas Nuclear Corp. Publication No. 5845 (1962).

2. C. K. Li, K. W. Wenzel, R. D. Petrasso *et al.* submitted to Rev. Sci. Instrum. (1992).

3. J. W. Coleman, K. W. Wenzel, C. K. Li *et al.*, Rev. Sci. Instrum. **61**, 3234 (1990).

4. To measure low-energy D-D $^3$He particles with VSBD, we use either a 0.5 $\mu$m mylar filter and maintain the beam voltage at $\lesssim$40 kV, or no filter and maintain the beam voltage at $\lesssim$25 kV in order to reduce backscattered beam counts in the VSBD.

5. D. H. Lo, R. D. Petrasso, K. W. Wenzel *et al.*, submitted to Rev. Sci. Instrum. (1992).

6. M. J. Loughlin, J. M. Adams, and G. Sadler, Nucl. Instrum. and Meth. **A294**, 606 (1990).

7. K. W. Wenzel, R. D. Petrasso, D. H. Lo *et al.*, submitted to Rev. Sci. Instrum. (1992).

Table 1: D-D neutron energies, calculated (on the basis of beam/target kinematics and neutron scattering on $^3$He) and measured (with a $^3$He proportional counter; all in MeV). The measured values agree to <5% with the predictions

| $\theta$ | Measured Full Energy | Predicted Full Energy | Measured Recoil Edge | Predicted Recoil Edge |
|---|---|---|---|---|
| 40° | 3.57 | 3.60 | 1.92 | 2.13 |
| 90° | 3.23 | 3.25 | 1.69 | 1.87 |
| 140° | 3.01 | 2.95 | 1.58 | 1.64 |

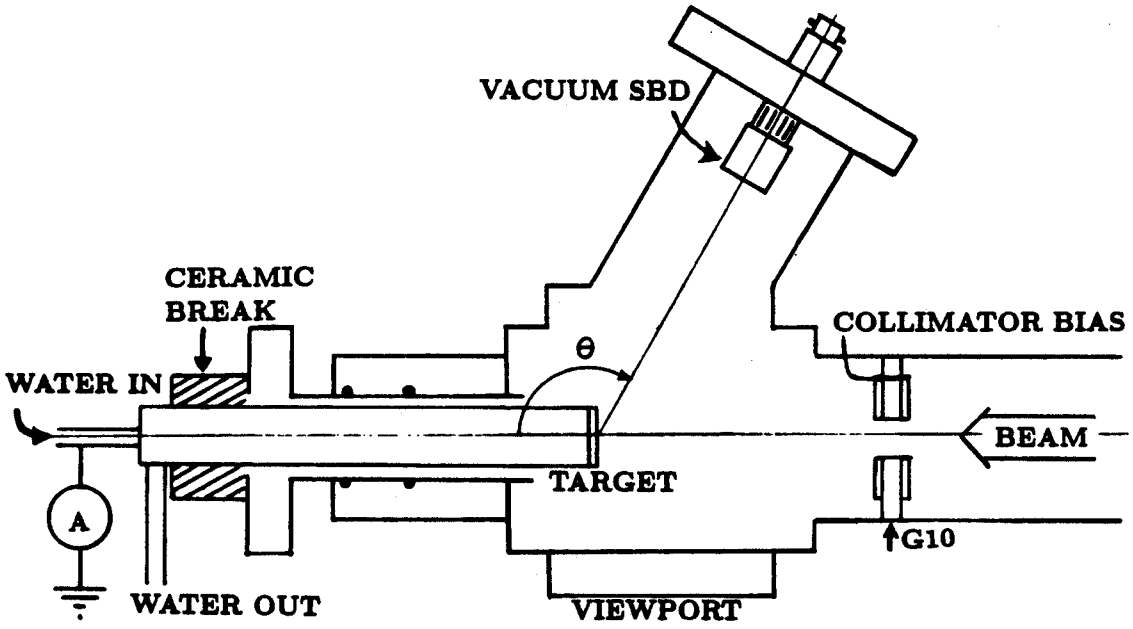


Fig. 1. Schematic diagram of the target chamber. The water-cooled target and the collimator are positively biased to restrain secondary electrons from leaving. The beam current on target is measured directly. A surface barrier diode at angle $\theta$ is operated in vacuum to detect charged fusion products.

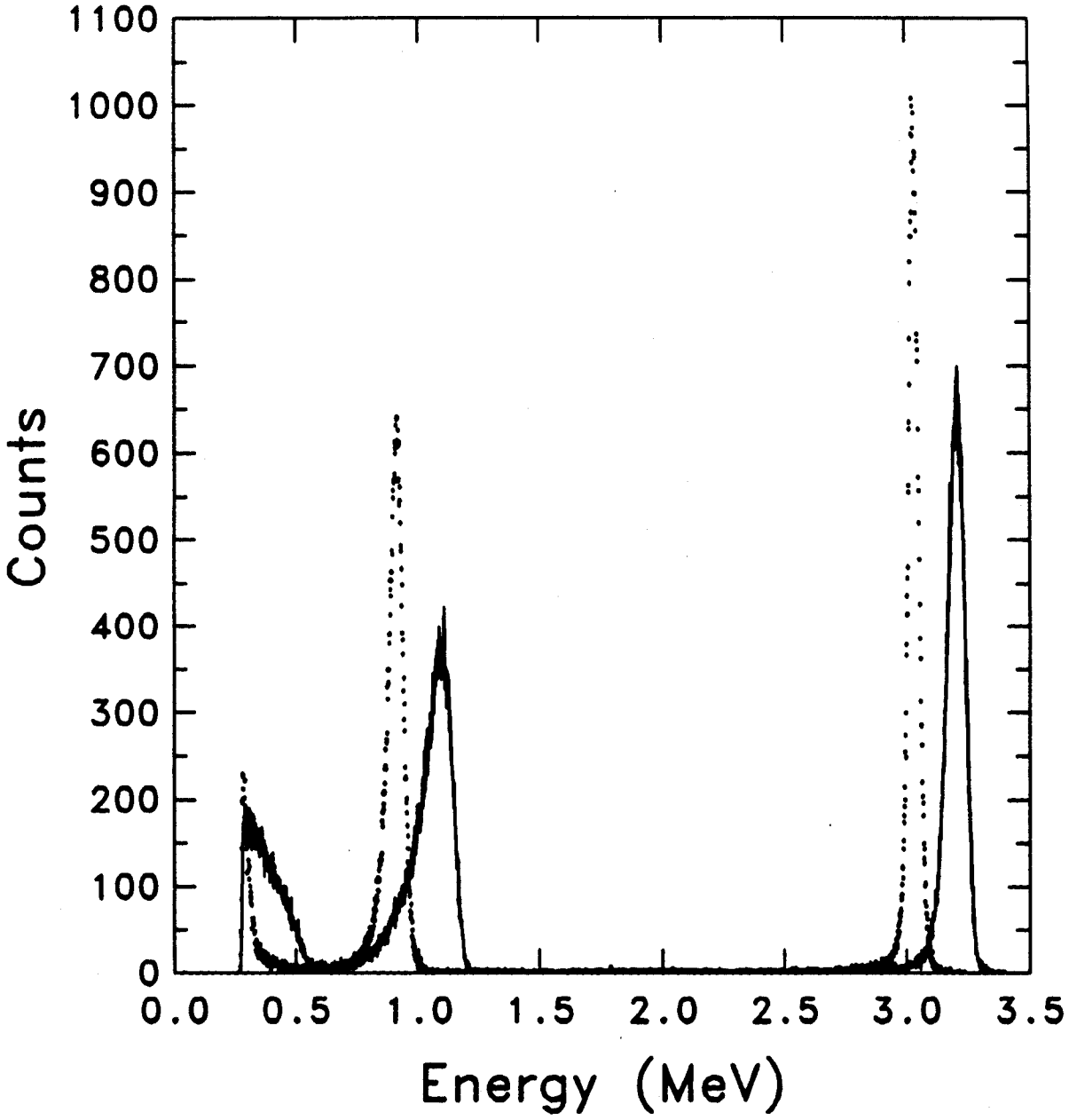


Fig. 2. D-D charged-particle spectra were measured with a vacuum SBD at $\theta \simeq 65°$ (solid spectrum) and $\theta \simeq 115°$ (dotted spectrum). Higher energies were measured when the SBD viewed the target from a "forward" angle (*i.e.*, $\theta \leq 90°$).

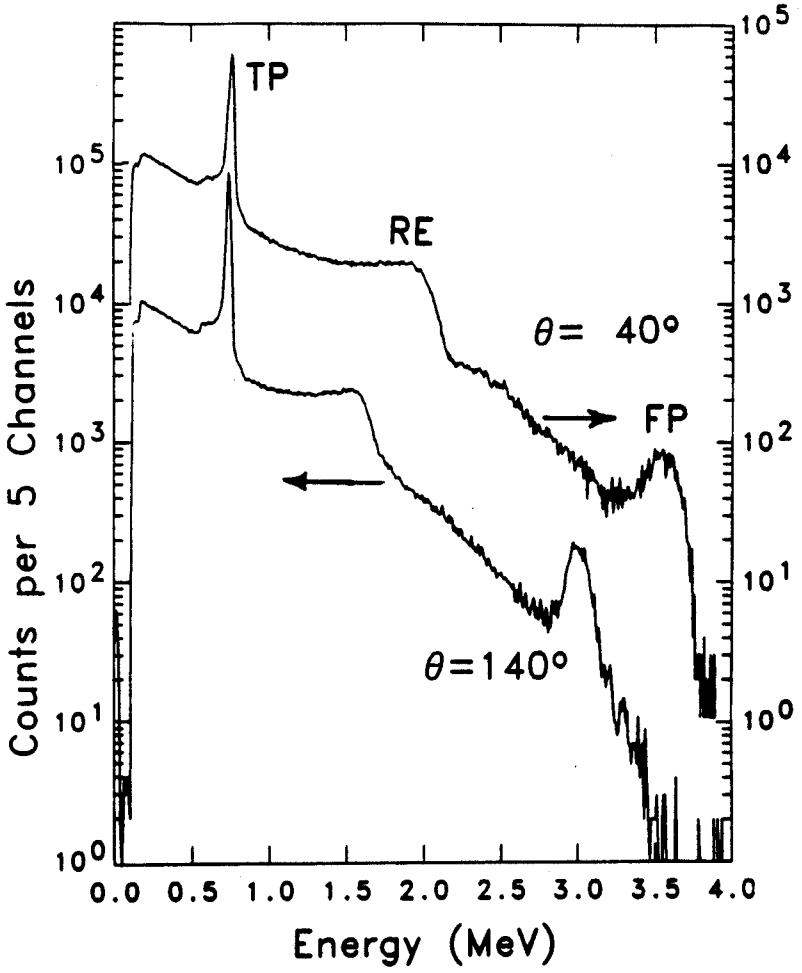


Fig. 3. $^3$He proportional-counter fast-neutron spectra were measured at $\theta \simeq 40°$ and $\theta \simeq 140°$. An energy calibration was obtained by using the thermal capture peak (at 765 keV) and the lowest edge due to the wall effect (at 191 keV). The "fast peak" (FP) and the recoil edge (RE) are at higher energies for forward angles (see Table 1).

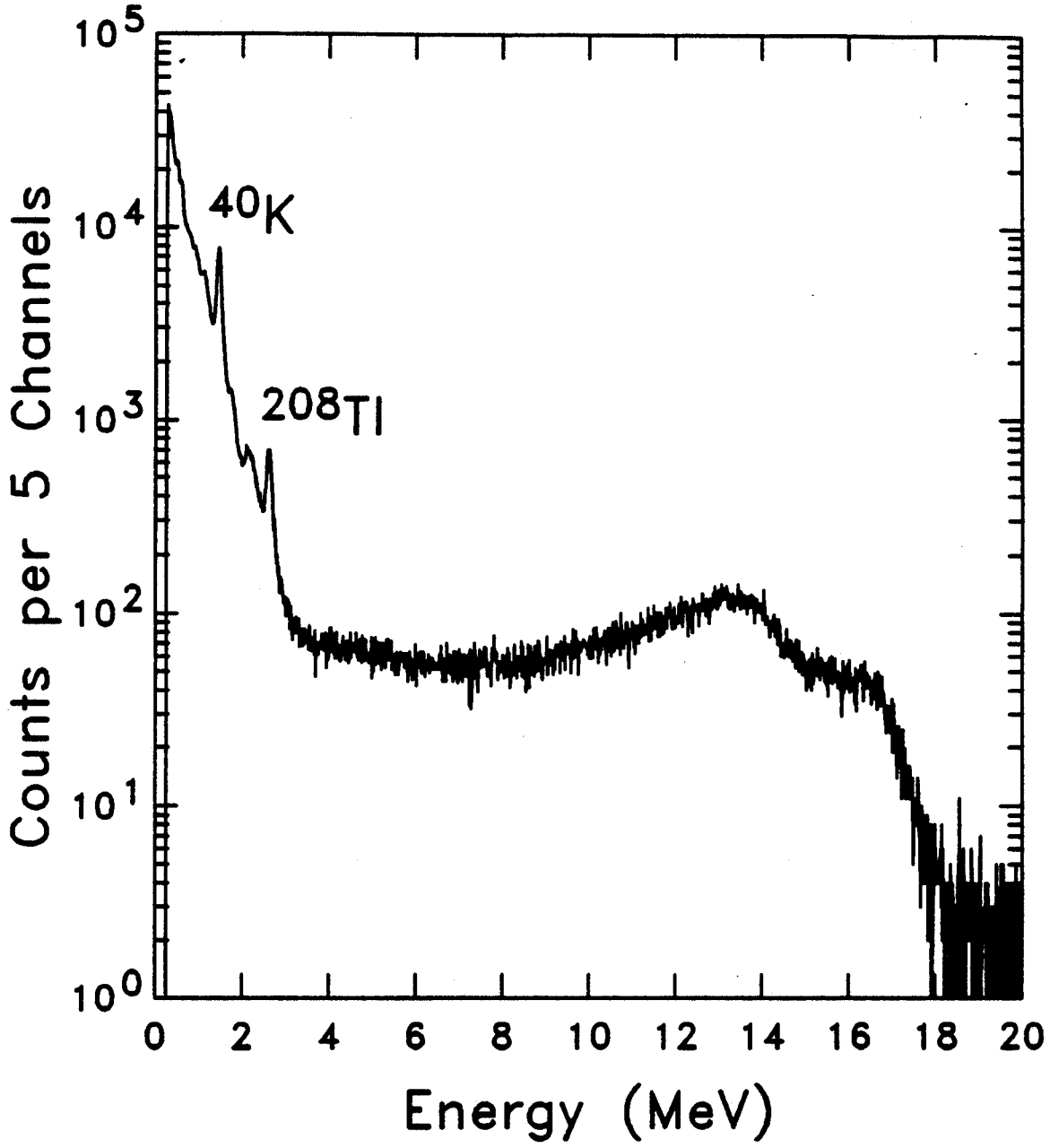


Fig. 4. The $\gamma$ rays (at 17.3 and 14 MeV) from the $^{7}$Li(p,$\gamma$)$^{8}$Be reaction were measured with a 3" $\times$ 3" NaI(Tl) scintillator. A natural lithium target was used, but the 5.6-MeV $^{6}$Li(p,$\gamma$)$^{7}$Be $\gamma$ rays were not observed in the NaI(Tl) data because of the small $\gamma$-ray branching ratio. (The background lines of $^{40}$K and $^{208}$Tl are also present at 1.46 MeV and 2.61 MeV respectively.)